ORIGINAL ARTICLE

Cellular uptake of poly(DL-lactide-co-glycolide) nanoparticles: effects of drugs and surface characteristics of nanoparticles

Sang Seung Lee[1] · Yong Bok Lee[1] · In Joon Oh[1]

Abstract In general, nanoparticles are internalized into cells by endocytosis. In the present study, we examine the cellular uptake of poly(lactic-co-glycolic) (PLGA) nanoparticles according to the hydrophilicity of the incorporated drug. Rhodamine B was used as a hydrophilic drug model and coumarin 6 as a hydrophobic drug model, both of which had fluorescent characteristics. The cellular uptake of the drug-loaded PLGA nanoparticles prepared by the solvent evaporation method was examined by flow cytometry and confocal microscopy. Rhodamine B could not pass through the membrane of HEK293 cells, however, rhodamine B-loaded PLGA nanoparticles could enter cells more easily. Conversely, both coumarin 6 and coumarin 6-loaded PLGA nanoparticles were observed inside cells, however, a higher fluorescence intensity was seen with coumarin 6-loaded PLGA nanoparticles in HEK293 cells than that of coumarin 6 alone. In order to investigate the nanoparticle uptake by cells, a fluorescent amine-PLGA (FA-PLGA), a PLGA polymer covalently bound directly to fluoresceinamine, was synthesized and observed inside cells by flow cytometry and confocal microscopy. The fluorescence of coumarin 6-loaded PLGA nanoparticles coated with chitosan was detected at the surface of cells, suggesting a charge interaction of the positive chitosan/PLGA nanoparticles with the negative cell membrane. This study presents the uptake of hydrophilic and hydrophobic nanoparticles in HEK293 cells.

Introduction

Nanoparticulate drug delivery systems have emerged as one of the most promising strategies to achieve a controlled and site-specific drug delivery. Polymer nanoparticles for therapeutic delivery are of particular interest due to their biocompatibility, biodegradability, and ability to maintain therapeutic drug levels for sustained periods of time (Cartiera et al. 2009). Poly(D,L-lactide-co-glycolide) (PLGA) polymers are usually used in the preparation of these carriers, owing to their biodegradability, biocompatibility, and FDA approval.

Therapeutic targets are located at intracellular sites, thus drug carriers should be able to easily cross the cell membrane. As a result, there needs to be a clear understanding of the interaction between nanoparticles and cells. Nanoparticles are easily internalized into cells through association with the cell membrane. In particular, endocytic uptake is the main route for the internalization of drug-loaded nanoparticles into cells. The cellular uptake characteristics of nanoparticles change according to size, shape, surface charge, surface functional groups, and hydrophilicity of nanoparticles (Kettler et al. 2014). In general, nanoparticles smaller than 500 nm are internalized into cells by a non-phagocytic pathway. Win and Feng (2005) showed that nanoparticles of 100–200 nm in size have a higher level of cellular uptake than those that are larger.

In order to detect the uptake of nanoparticles, fluorescent dye has been used as a fluorescence probe to analyze the efficiency of nanoparticle localization in a particular

✉ In Joon Oh
ijoh@jnu.ac.kr

[1] College of Pharmacy, Chonnam National University, 77 Yongbong-ro, Gwangju 61186, Korea

cell population. It is important that the marker is incorporated into the nanoparticles at a sufficient level to give good detection by the analytical methods used. Flow cytometry can evaluate the characteristics of many cells very quickly, but cannot give exact information regarding the localization of nanoparticles in the cells. Confocal microscopy overcomes this limitation with its superior spatial resolution (Torrano et al. 2013).

Since studies relating to nanoparticles began, many drug-loaded nanoparticles have been prepared using PLGA polymers and studied in various fields. However, comparative studies concerning hydrophilicity and hydrophobicity have not yet been established, despite the fact that the physicochemical properties of all drugs can be classified into these two groups. Rhodamine B may be an excellent choice as a model for hydrophilic drugs due to its red fluorescence and high solubility in water, thus rhodamine B-loaded PLGA nanoparticles are suitable for the investigation into the distribution of hydrophilic drugs (Essa et al. 2011). Coumarin compounds have been used as fluorescent brighteners, laser dyes, and organic nonlinear optical materials in the 'blue–green' region (Bhattacharyya et al. 2011). Accordingly, here, we employ coumarin 6 as a fluorescent probe molecule to investigate the nanoenvironment characteristics of hydrophobic drugs.

The surface charge of nanoparticles, in particular a positive charge, influences the efficiency of cellular uptake. Nanoparticles with a positive zeta-potential can associate with the negative constituents of the cell membrane (Chiu et al. 2010). Here, we introduce chitosan in order to change the surface charge of PLGA nanoparticles.

In the present study, the drug release and uptake characteristics of rhodamine B- or coumarin 6-loaded PLGA nanoparticles are evaluated under various conditions. Dye-loaded PLGA nanoparticles were prepared by the solvent evaporation method, and the zeta-potential and drug content were measured. Drug release in phosphate buffered solution at pH 4.0 and 7.4 were also evaluated. In addition, we measured the cellular uptake of hydrophilic rhodamine B and hydrophobic coumarin 6 in human embryonic kidney (HEK) 293 cells using flow cytometry and confocal microscopy.

Materials and methods

Materials

Rhodamine B, fluorescent amine (FA), 1-ethyl-3-(3-dimethylaminopropyl)-carbodiimide hydrochloride (EDC), coumarin 6, polyvinyl alcohol (PVA) (87–89 % hydrolyzed, Mw 13–23 kDa), PLGA (Mw = 50,000–75,000), and chitosan (75–85 % deacetylation, 20–200 cps) were

obtained from Sigma-Aldrich (USA). All the solvents and other reagents were of analytical grade.

Conjugation of PLGA to fluorescent amine

FA-PLGA was prepared by the method described by Horisawa et al. (2002), with slight modifications. Briefly, 600 mg PLGA and 0.0116 g FA were dissolved in 6 ml acetonitrile with 0.008 g EDC. The reaction mixture was stirred for 2 h at room temperature, and then washed with distilled water followed by drying.

Preparation of PLGA nanoparticles

PLGA nanoparticles were prepared by an emulsification solvent evaporation method (Park et al. 2008). To prepare rhodamine B- or coumarin 6-loaded PLGA nanoparticles, 200 mg PLGA polymer was dissolved in 8 ml methylene chloride and mixed with 1.6 ml rhodamine B solution (10 mg) or 10 mg coumarin 6, followed by emulsification using a sonicator for 3 min. This w/o emulsion (rhodamine B in PLGA solution) or methylene chloride solution (coumarin 6 and PLGA) was mixed with 16 ml 2 % PVA solution and sonicated for 5 min. This emulsion was added dropwise to 80 ml 0.6 % PVA solution. Stirring of the emulsion was carried out for 10 min using a magnetic stirrer at room temperature. Methylene chloride was evaporated under reduced pressure using a rotary evaporator for 40 min. Subsequently, the PLGA nanoparticle suspension was centrifuged at 17,000 rpm for 30 min, and then washed with distilled water. Centrifugation and washing steps were repeated twice. The washed nanoparticle suspension was lyophilized and stored at 4 °C until further use.

Preparation of chitosan-coated PLGA nanoparticles

For the preparation of coumarin 6-loaded PLGA nanoparticles coated with chitosan, adsorption of chitosan onto the PLGA nanoparticles was carried out. Briefly, 5 ml 0.1 % chitosan solution was added to 40 ml coumarin 6-loaded PLGA nanoparticle (40 mg) suspension and gentled stirred for 5 h (Yang et al. 2009). Finally, this suspension was centrifuged at 12,000 rpm for 20 min and washed with distilled water. This procedure was repeated twice and lyophilized.

Physicochemical characterization of nanoparticles

The drug content and loading efficiency of nanoparticles were analyzed using a UV spectrophotometer (Specgene, Techne, UK). The concentrations of rhodamine B and coumarin 6 were detected by UV absorbency at 555 and

444 nm, respectively. The average particle size and zeta-potential of the nanoparticles dispersed into distilled water were measured using an electrophoretic light scattering analyzer (ELS-8000, Otsuka, Japan).

Release characterization in vitro

Drug release in vitro was performed using the dialysis bag (MW cut-off = 12,000) diffusion technique. Nanoparticles (10 mg) suspended in 1 ml buffer solution (pH 4 or 7.4) were placed in a hermetically sealed dialysis bag and introduced into a Falcon tube with 10 ml phosphate buffered saline (PBS) as a release medium. The release experiment was performed at 37 °C with a shaking rate of 100 rpm in a shaking incubator. The entire volume of release medium was taken at predetermined time intervals to maintain the sink conditions. Released amounts of rhodamine B and coumarin 6 were measured using a UV spectrophotometer at a wavelength of 555 and 444 nm, respectively.

Assessment of cellular uptake by flow cytometry and confocal microscopy

HEK293 cells were grown at 37 °C and 5 % carbon dioxide in Dulbecco's modified Eagle medium (DMEM) supplemented with 10 % fetal bovine serum and 1 % Antimycin in cell culture dishes (100 mm × 20 mm). Fluorescence analysis was performed using a fluorescence activated cell sorting (FACS) analyzer (Calibur, Biosciences, USA) and a laser scanning confocal microscope (LSCM) (TCS SP5, Leica, Germany). The cells were routinely passaged at 90–95 % confluence for FACS, and 40–50 % for confocal microscopy. Firstly, the DMEM used to incubate HEK293 cells was removed and the cells were washed once with PBS. Cells were treated with DMEM solutions (0.1 mg/ml) dispersed with nanoparticles and incubated for 4 h at 37 °C in an atmosphere of 5 % carbon dioxide. For FACS and confocal analysis, the quantities of each drug and nanoparticles were uniformly adjusted to 0.1 mg/ml. The fluorescence intensity of rhodamine B in FACS was measured after treating the cells for 1, 2, and 4 h. The fluorescence intensity of coumarin 6 or fluorescent amine was measured after treating the cells for 1 and 4 h. After treatment with the samples for 4 h, the cells were imaged using a confocal microscope.

Statistical analysis

All the experiments were performed at least three times, and statistically significant differences between treatments were calculated using student's t test or ANOVA test (SPSS version 21).

Results and discussion

Physicochemical properties of nanoparticles

Due to the hydrophilic characteristics of rhodamine B, the w/o/w emulsion-solvent evaporation method was chosen for the preparation of rhodamine B-loaded PLGA nanoparticles. The w/o/w method was able to load 6–10 times more rhodamine B than the o/w emulsion method. Hydrophobic coumarin 6 was encapsulated in PLGA nanoparticles using the w/o emulsion-solvent evaporation method. Table 1 shows the drug content and loading efficiency of rhodamine B/PLGA and coumarin 6/PLGA nanoparticles. The loading efficiencies of rhodamine B and coumarin 6 were approximately 12 and 52 %, respectively, with the encapsulation of hydrophilic rhodamine being much lower than coumarin 6. This is likely due to the enhanced diffusion of hydrophilic rhodamine B out of the emulsion droplets during the production of the nanoparticles. Conversely, coumarin 6 was loaded efficiently into the polymer. The physicochemical properties of the drugs had a great influence on drug loading into the polymer nanoparticles.

The size and zeta-potential of rhodamine B/PLGA, coumarin 6/PLGA, coumarin 6/PLGA coated with chitosan, and rhodamine B/FA-PLGA nanoparticles are shown in Table 2. The size range of the nanoparticles was found to be 150–200 nm, with the exception of the chitosan-coated PLGA nanoparticles, of which the size was very large (almost 800 nm) in comparison with the other three nanoparticles. The large size of the chitosan-coated PLGA nanoparticles was a result of the firm adsorption of chitosan onto the surface of PLGA nanoparticles by ionic interaction. The zeta-potential of rhodamine B/PLGA, coumarin 6/PLGA, and rhodamine B/FA-PLGA nanoparticles was −61.8, −47.8 and −8.6 mV, respectively. The negative zeta-potential of these nanoparticles may originate from the functional residue of PLGA, especially the carboxyl group. Due to the cationic characteristics of the amine group in the fluoresceinamine molecule, the absolute value for the zeta-potential of rhodamine B/FA-PLGA nanoparticles was lower than that of the rhodamine B/PLGA nanoparticles. The zeta-potential of chitosan-coated PLGA nanoparticles counteracted the negative charge and reversed it to +3.43 mV as a result of the adsorption of the polycationic chitosan polymer onto the surface of the coumarin 6/PLGA nanoparticles.

In vitro release of nanoparticles

The release of rhodamine B and coumarin 6 from PLGA nanoparticles was determined at pH 7.4 and 4.0. Since

Table 1 Drug contents and loading efficiency of rhodamine B/PLGA and coumarin 6/PLGA nanoparticles

| Drug-loaded nanoparticle	Drug contents (wt%)	Load efficiency (wt%)
Rhodamine B/PLGA	0.75 ± 0.28	12.26 ± 4.62
Coumarin 6/PLGA	3.27 ± 0.02	52.03 ± 2.51

Table 2 Size and zeta-potential of nanoparticles

Nanoparticle	Particle size (nm)	Zeta-potential (mV)
Rhodamine B/PLGA	195 ± 15	−61.8 ± 15.5
Coumarin 6/PLGA	187 ± 32	−47.8 ± 23.3
Coumarin 6/chitosan-PLGA	783 ± 58	+3.4 ± 2.5
Rhodamine B/FA-PLGA	175 ± 26	−8.6 ± 5.4

nanoparticles are trafficked through an acidic endo-lyso-somal compartment at pH 4–5, it is necessary to test the release in acidic pH conditions (Panyam et al. 2003). Release patterns of the nanoparticles showed a typical profile of the initial burst effect and slow rate of release as shown in Fig. 1. Rhodamine B showed a fast release due to its high hydrophilicity. The cumulative released amounts of rhodamine B over 24 h were 80 % at pH 7.4 and 78 % at pH 4.0, respectively, and there was little difference between the two graphs at each pH. Conversely, approximately 5 % of coumarin 6 was released at pH 7.4 over 12 days compared with roughly 3 % release at pH 4.0 for the same period of time, but there were statistically insignificant differences between them by student's t test. Hydrophobic coumarin 6 was hardly released from the PLGA nanoparticles at pH 7.4 or 4.0.

Cellular uptake analysis by flow cytometry

Generally, nanoparticles are internalized into cells by pinocytosis pathways such as macropinocytosis, clathrin-mediated endocytosis, caveolae-mediated endocytosis, and mechanisms independent of clathrin and caveolae (Treuel et al. 2013). In addition, the uptake efficiency of nanoparticles is known to be dependent on their size, shape, surface charge, and surface chemistry. We analyzed the nanoparticle uptake in HEK293 cells using flow cytometry and confocal microscopy. The histogram plot of the FACS shows the fluorescence or light scatter intensity against the number of cells. In the flow cytometry graph, the x-axis is the intensity of fluorescence and the y-axis is the cell count. The gross area represents the total cell count. On the x-axis, FL1-H is used for the green fluorescence wavelength and FL2-H for the red fluorescence wavelength. Therefore, when the fluorescence of rhodamine B and coumarin 6 was measured, the FL2-H and
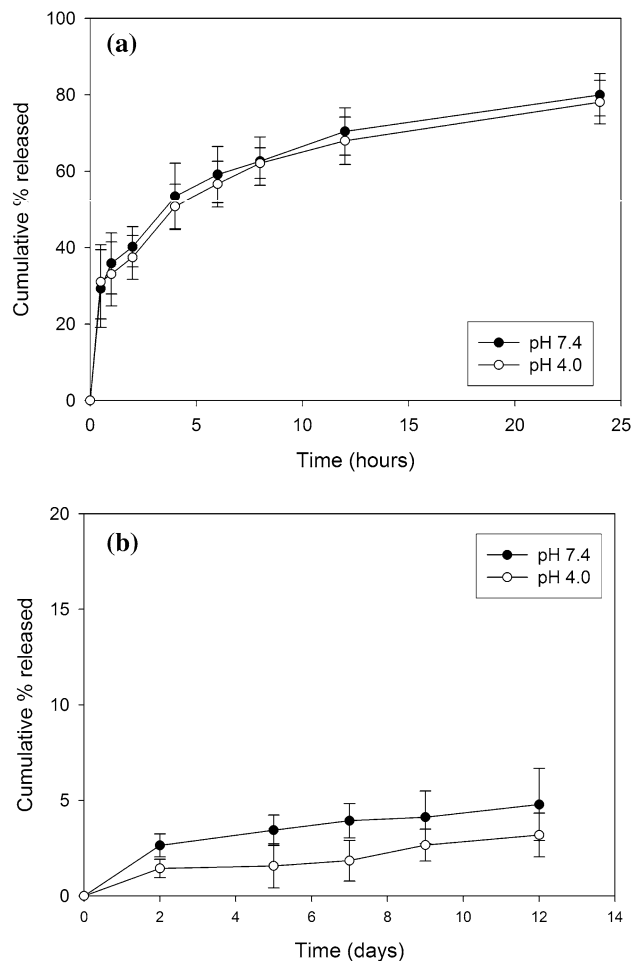

Fig. 1 Release profiles of **a** rhodamine B/PLGA and **b** coumarin 6/PLGA nanoparticles in pH 7.4 and 4.0 buffer at 37 °C (n = 3)

FL1-H wavelength was used, respectively. Figure 2 shows the FACS graphs of rhodamine B and rhodamine B/PLGA nanoparticles. The histogram colored black in Fig. 2a represents the fluorescence intensity of the unstained cells without any treatment. The fluorescence intensity of the samples treated with rhodamine B for 1, 2, and 4 h did not differ from the control. No shift of peaks in the case of the rhodamine B solution indicated that rhodamine B did not penetrate the cell membrane. However, the histograms of the rhodamine B/PLGA nanoparticles showed a peak shift to the right, which increased with an increase in incubation time as shown in Fig. 2b. This result implies uptake of the nanoparticles by the cells. In fact, rhodamine B is very

Fig. 2 a Flow cytometry distribution of rhodamine B fluorescence intensity after incubation with rhodamine B and **b** rhodamine B/PLGA nanoparticles in HEK293 cells for 1, 2, and 4 h. **c** The mean fluorescence intensity of rhodamine B after incubation with rhodamine B/PLGA nanoparticles. One-way ANOVA $p < 0.001$, $F(3,8) = 54.8$; Paired t test: $*p < 0.05$ and $**p < 0.01$
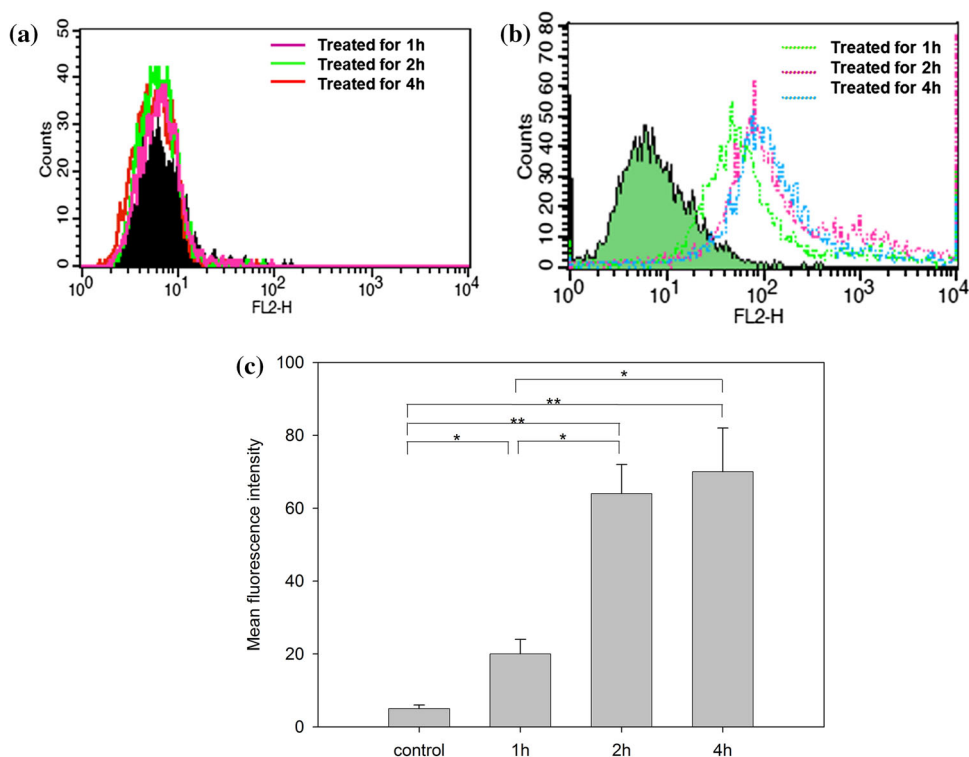
hydrophilic, and thus hardly passed across the hydrophobic cell membrane, while the rhodamine B-loaded PLGA nanoparticles could be internalized into the cells by endocytosis. Figure 2c shows the mean fluorescence intensity of rhodamine B/PLGA nanoparticles according to the cell incubation time. The increase in fluorescence intensity of the rhodamine B/PLGA nanoparticles with incubation time indicates the time-dependent transfer of the hydrophilic drug-loaded nanoparticles into the cells. Conversely, the fluorescence intensity of coumarin 6 in HEK293 cells increased as shown in Fig. 3a. The passage of coumarin 6 through the cell membrane can be inferred from the hydrophobicity of coumarin 6. As the hydrophobic drugs were internalized into cells by passive diffusion, which had time-dependent characteristics, the fluorescence intensity of coumarin 6 increased with incubation time. When coumarin 6 was loaded into the PLGA polymer, the fluorescence intensity of coumarin 6/PLGA was higher than that of coumarin 6 alone. This fact indicates that the coumarin 6/PLGA nanoparticles can be internalized into the cells more efficiently than coumarin 6 only. From the results of the mean fluorescence intensity, the uptake profile of the coumarin 6/PLGA nanoparticles treated for 4 h was similar to that of those treated for 1 h (Fig. 3b). Since the release of coumarin 6 from the nanoparticles was very low, the high fluorescence intensity of the coumarin 6/PLGA nanoparticles was due to the uptake of the PLGA nanoparticles by endocytosis. According to Xu et al. (2009), nanoparticles encapsulated with very hydrophobic
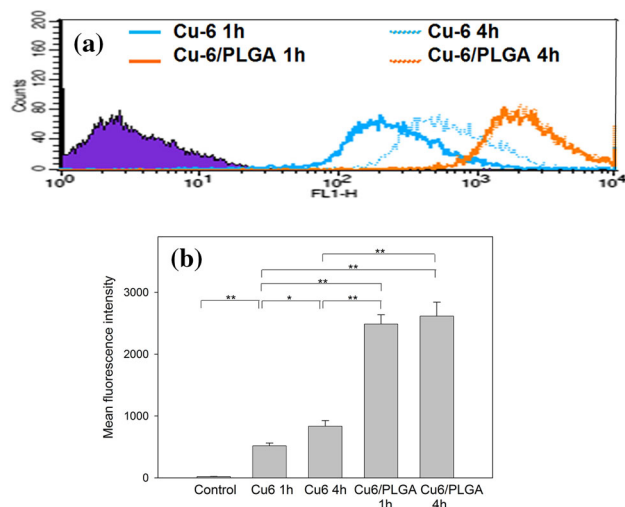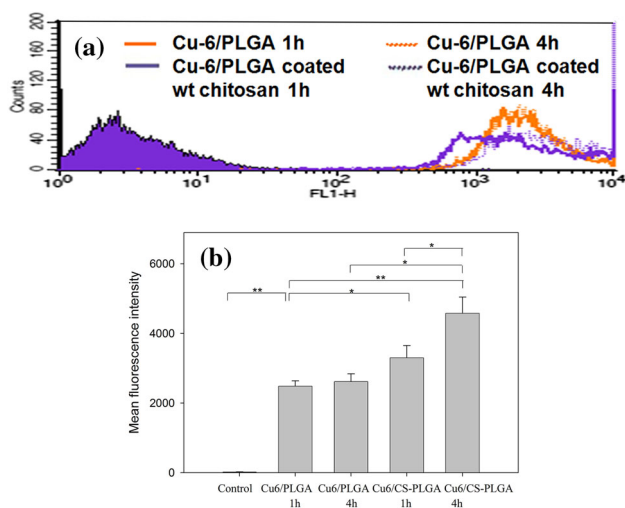
Fig. 3 a Flow cytometry distribution of coumarin 6 fluorescence intensity after incubation with coumarin 6 and coumarin 6/PLGA nanoparticles in HEK293 cells for 1 and 4 h. **b** The mean fluorescence intensity of coumarin 6 after incubation with coumarin 6 and coumarin 6/PLGA nanoparticles. One-way ANOVA $p < 0.001$, $F(4,10) = 251.6$; Paired t test: $*p < 0.05$ and $**p < 0.01$

drugs were internalized directly into cells or released the drugs at the cell surface.

To investigate the cellular uptake of PLGA nanoparticles, a FA-PLGA conjugate, the covalent bonding of a PLGA polymer to a fluorescence amine, was used. The fluorescence intensity of the fluorescent amine was examined upon loading of the cells for 1 or 4 h with FA-PLGA
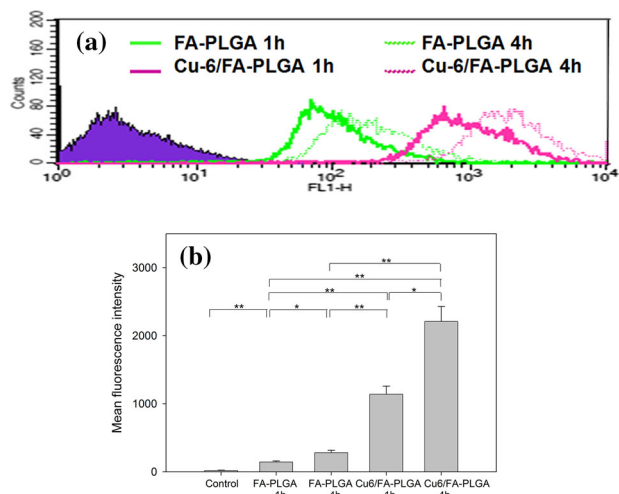
Fig. 4 a Flow cytometry distribution of FA and coumarin 6 fluorescence intensity after incubation with FA-PLGA and coumarin 6/FA-PLGA nanoparticles in HEK293 cells for 1 and 4 h. b The mean fluorescence intensity of FA and coumarin 6 after incubation with FA-PLGA and coumarin 6/FA-PLGA nanoparticles. One-way ANOVA $p < 0.001$, $F(4,10) = 198.6$; Paired t test: *$p < 0.05$ and **$p < 0.01$

Fig. 5 a Flow cytometry distribution of coumarin 6 fluorescence intensity after the incubation with coumarin 6/PLGA and coumarin 6/PLGA coated with chitosan in HEK 293 cells for 1 and 4 h. b The mean fluorescence intensity of coumarin 6 after the incubation of coumarin 6/PLGA and coumarin 6/PLGA coated with chitosan. One-way ANOVA $p < 0.001$, $F(4,10) = 101.6$; Paired t test: *$p < 0.05$ and **$p < 0.01$

nanoparticles, with or without coumarin 6, as shown in Fig. 4a. The presence of fluorescence within cells indicates that the PLGA nanoparticles can be internalized very easily. The excitation and emission wavelengths of coumarin 6 are 387 and 505 nm, respectively, while those of
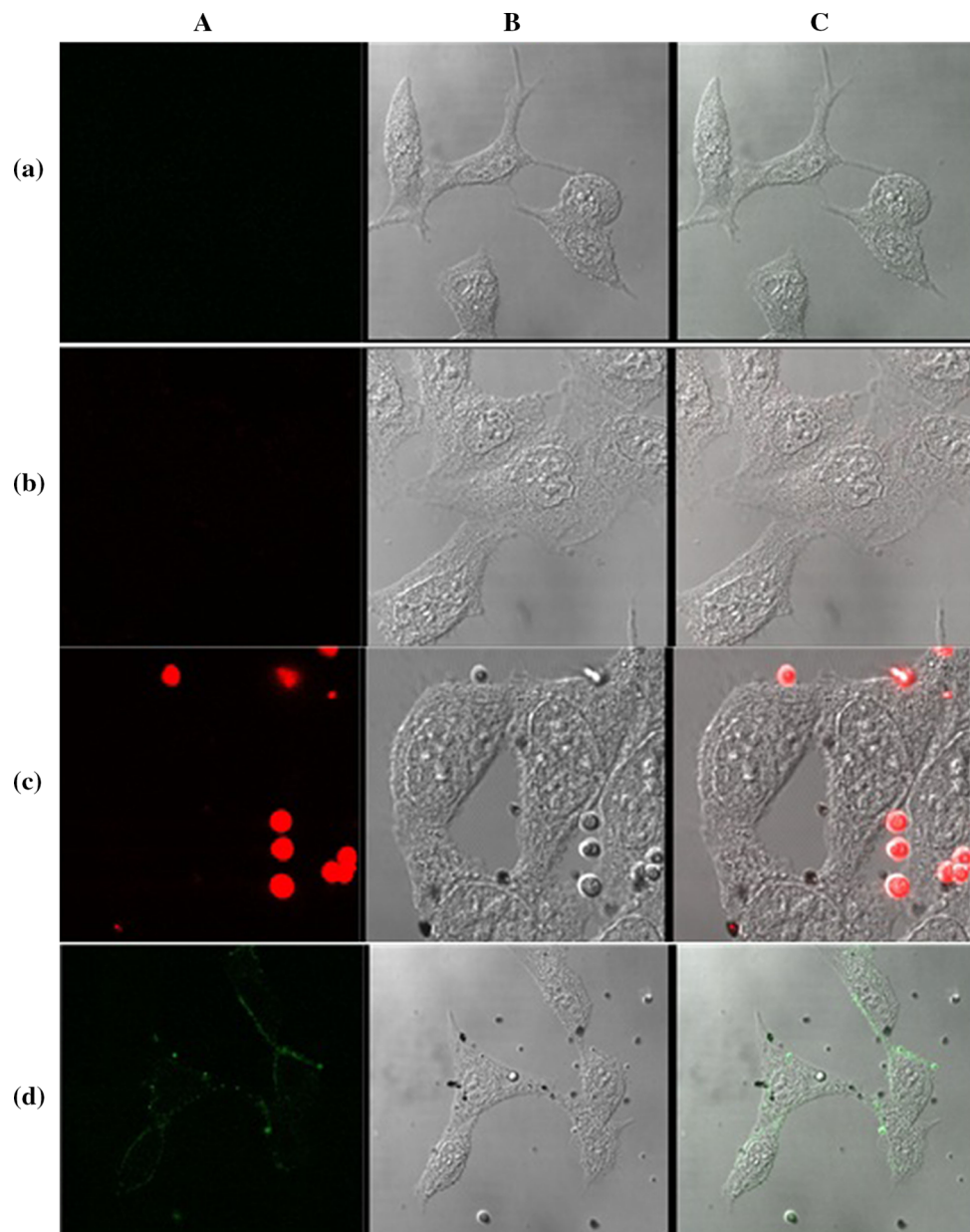
the fluorescent amine are 490 and 525 nm, respectively. Due to the fact that the emission wavelength of the two dyes overlaps in the range of the FL1-H green wavelength, a higher fluorescence intensity will be detected with the coumarin 6-loaded FA-PLGA nanoparticles than the blank FA-PLGA nanoparticles, if both FA and coumarin 6 are taken up by the cells. The higher fluorescence intensity of the coumarin 6/FA-PLGA nanoparticles compared with the FA-PLGA nanoparticles confirms this hypothesis, as shown in Fig. 4b.

Generally, nanoparticles with a positive surface charge are taken up in non-phagocytic cells to a high extent due to the high interaction between the nanoparticles and the cell membrane (Fröhlich 2012). We evaluated the uptake of chitosan/PLGA nanoparticles with a positive surface zeta-potential in HEK293 cells. The fluorescence of coumarin 6/PLGA nanoparticles coated with chitosan was detected by flow cytometry as shown in Fig. 5a. The peak of the coumarin 6/PLGA nanoparticles coated with chitosan moved to the right with increasing incubation time. Since particle size affects the intracellular uptake of nanoparticles (Kettler et al. 2014), larger particles would have a lower uptake than smaller ones. However, the larger chitosan-coated PLGA nanoparticles exhibited a higher mean fluorescence intensity than the PLGA nanoparticles (Fig. 5b). This result suggests that chitosan-coated PLGA nanoparticles may accumulate at the membrane due to the electrostatic interaction between the positive surface charge of the nanoparticles and the negative charge of the cell membrane, which facilitated a higher concentration of coumarin 6 at the membrane surface (Do et al. 2008).

Confocal microscopy analysis

The cellular uptake of dye-loaded PLGA nanoparticles can be easily visualized by confocal microscopy. Figures 6 and 7 distinctly present the fluorescence images by confocal microscopy of rhodamine B and coumarin 6 in HEK293 cells, respectively, after treatment for 4 h. The left image shows fluorescence, the middle image indicates the morphology of the treated cells, and the right image is the two merged images. Control cells (Fig. 6a) and cells treated with rhodamine B (Fig. 6b) did not exhibit fluorescence, whereas cells treated with the rhodamine B/PLGA nanoparticles (Fig. 6c) exhibited red fluorescence. The PLGA nanoparticles localized in vesicles after endocytosis, as seen by spots of cellular fluorescence. These observations strongly support the notion that the hydrophilic rhodamine B alone does not pass through the cell membrane, while the rhodamine B-loaded nanoparticles can be internalized into cells easily. These results are consistent with the data obtained by flow cytometry. Figure 6d shows a small number of fluorescent spots of FA-PLGA nanoparticles without loading dye,

which is definite evidence of the uptake of PLGA nanoparticles.

The green fluorescence of coumarin 6 in cells was detected as shown in Fig. 7a, indicating that coumarin 6 could pass through the cell membrane. The coumarin 6/PLGA nanoparticles also emitted green fluorescence as shown in Fig. 7b. In this figure, the green fluorescence of the coumarin dye appears as a bright dot over the entire domain of cells. The coumarin 6/PLGA nanoparticles coated with chitosan surround the outer membrane of HEK293 cells as shown in Fig. 7c. This is evidence of the interaction between the positive chitosan and the negative cell membrane. The results of the confocal microscopy are consistent with the FACS results.

Conclusions

PLGA nanoparticles were prepared successfully by the solvent evaporation method. The size distribution ranged from 150 to 200 nm for all prepared PLGA nanoparticles, with the exception of the coumarin 6/PLGA nanoparticles coated with chitosan, which had a diameter of 800 nm. According to the FACS and LSCM results, rhodamine B, which was used as a hydrophilic drug model, could not penetrate the cell membrane, while the rhodamine B-loaded PLGA nanoparticles could easily enter HEK293 cells. Coumarin 6, which was used as a hydrophobic drug model, could penetrate the cell membrane, and was even more efficient in the case of coumarin-loaded PLGA

Fig. 7 Fluorescence image and morphology of HEK293 cells monitored by confocal microscopy. **a** Coumarin 6, **b** coumarin 6/PLGA nanoparticles and **c** coumarin 6/PLGA nanoparticles coated with chitosan. **A** Fluorescence, **B** morphology of treated cells, **C** the two merged images. *Scale bar* 10 μm
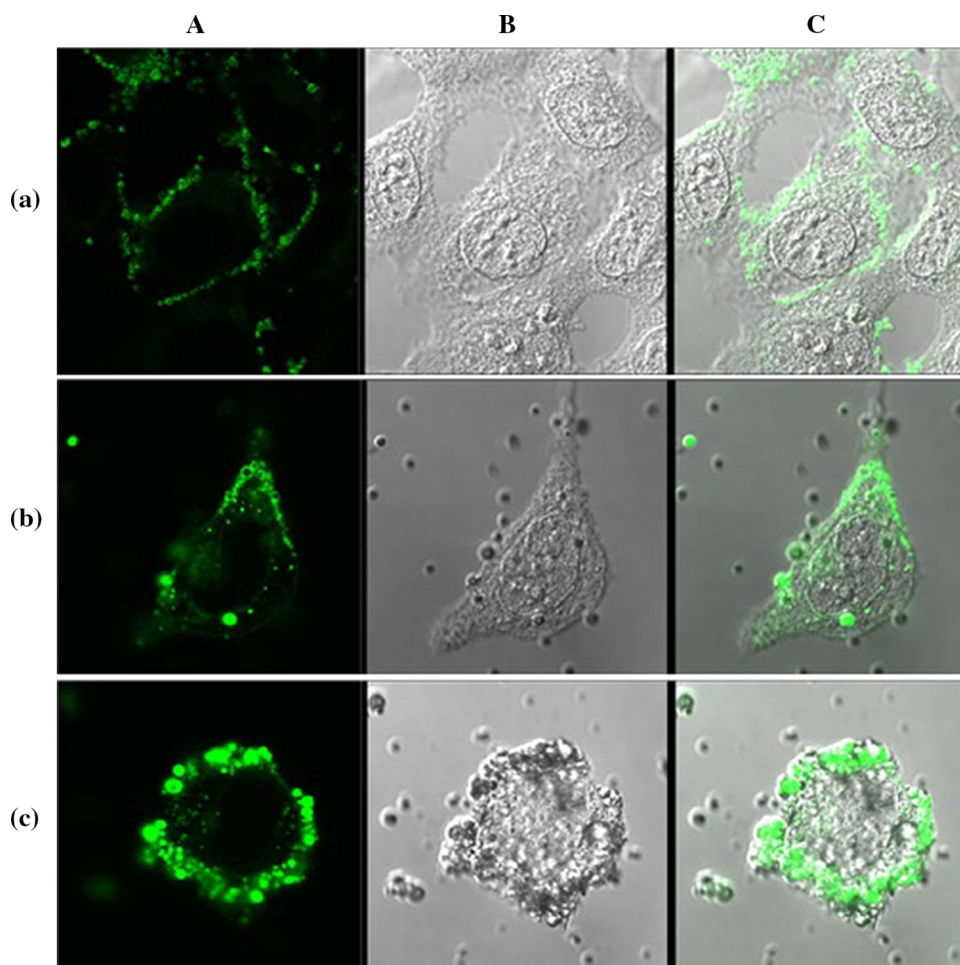
nanoparticles. FA-PLGA nanoparticles, directly conjugated along with a fluorescent amine to PLGA, could enter the cells, suggesting that the small nanoparticles were internalized into the cells by endocytosis. The coumarin 6/PLGA nanoparticles coated with chitosan were concentrated at the surface of the cells due to the interaction of the positive chitosan with the negative cell membrane. FACS and confocal microscopy analysis of PLGA nanoparticles suggests that drug-loaded PLGA nanoparticles entered cells by endocytosis or passive diffusion of a hydrophobic drug released from nanoparticles.

References

Bhattacharyya SS, Paul S, De A, Das D, Samadder A, Boujedaini N, Khuda-Bukhsh AR (2011) Poly(lactide-co-glycolide) acid nanoencapsulation of a synthetic coumarin: cytotoxicity and bio-distribution in mice, in cancer cell line and interaction with calf thymus DNA as target. Toxicol Appl Pharmacol 253:270–281

Cartiera MS, Johnson KM, Rajendran V, Caplan MJ, Saltzman WM (2009) The uptake and intracellular fate of PLGA nanoparticles in epithelial cells. Biomaterials 30:2790–2798

Chiu YL, Ho YC, Chen YM, Peng SF, Ke CJ, Chen KJ, Mi FL, Sung HW (2010) The characteristics, cellular uptake and intracellular trafficking of nanoparticles made of hydrophobically-modified chitosan. J Control Release 146:152–159

Do JH, An J, Joun YS, Chung DJ, Kim JH (2008) Cellular-uptake behavior of polymer nanoparticles into consideration of biosafety. Macromol Res 16:695–703

Essa S, Rabanel JM, Hildgen P (2011) Characterization of rhodamine loaded PEG-g-PLA nanoparticles: effect of poly(ethylene glycol) grafting density. Int J Pharm 411:178–187

Fröhlich E (2012) The role of surface charge in cellular uptake and cytotoxicity of medical nanoparticles. Int J Nanomed 7:5577–5591

Horisawa E, Kubota K, Tuboi I, Sato K, Yamamoto H, Takeuchi H, Kawashima Y (2002) Size-dependency of DL-lactide/glycolide copolymer particulates for intra-articular delivery system on phagocytosis in Rat Synovium. Pharm Res 19:132–139

Kettler K, Veltman K, Meent D, Wezel A, Hendriks AJ (2014) Cellular uptake of nanoparticles as determined by particle properties, experimental conditions, and cell type. Environ Toxicol Chem 33:481–492

Panyam J, Sahoo SK, Prabha S, Bargar T, Labhasetwar V (2003) Fluorescence and electron microscopy probes for cellular and tissue uptake of poly(D,L-lactide-co-glycolide) nanoparticles. Int J Pharm 262:1–11

Park YM, Shin BA, Oh IJ (2008) Poly(L-lactic acid)/polyethylen-imine nanoparticles as plasmid DNA carriers. Arch Pharm Res 31:96–102

Torrano A, Blechinger J, Osseforth C, Argyo C, Reller A, Bein T, Michaelis J, Bräuchle C (2013) A fast analysis method to quantify nanoparticle uptake on a single cell level. Nanomedicine 8:1815–1828

Treuel L, Jiang X, Nienhaus GU (2013) New views on cellular uptake and trafficking of manufactured nanoparticles. J R Soc Interface 10:20120939. doi:10.1098/rsif.2012.0939

Win KY, Feng SS (2005) Effects of particle size and surface coating on cellular uptake of polymeric nanoparticles for oral delivery of anticancer drugs. Biomaterials 26:2713–2722

Xu P, Gullotti E, Tong L, Highley CB, Errabelli DR, Hasan T, Cheng JX, Kohane DS, Yeo Y (2009) Intracellular drug delivery by poly(lactic-co-glycolic acid) nanoparticles, revisited. Mol Pharm 6:190–201

Yang R, Shim WS, Cui FD, Cheng G, Han X, Jin QR, Kim DD, Chung SJ, Shim CK (2009) Enhanced electrostatic interaction between chitosan-modified PLGA nanoparticle and tumor. Int J Pharm 371:142–147